Multi-Class Brain Tumor Classification with DenseNet Based Deep Learning Features and Ensemble of Machine Learning Approaches

Shakil Mahmud Shuvo(✉), Md. Farukuzzaman Faruk, Azmain Yakin Srizon, Tahsen Islam Sajon, S. M. Mahedy Hasan, Anirban Barai, A. F. M. Minhazur Rahman, and Md. Al Mamun

Department of Computer Science & Engineering,
Rajshahi University of Engineering & Technology, Rajshahi-6204, Bangladesh
{sshuvo.cse(✉), faarukuzzaman, azmainsrizon, sajon.tahsen, mahedycseruet, anirbanplabon, m.r.saurov, almamun00350}@gmail.com

Abstract. The timely and precise diagnosis of brain tumors is crucial in reducing mortality rates. Although Magnetic Resonance Imaging (MRI) is commonly used as a detection tool for brain tumors, the presence of unwanted regions in MRI and multi-class brain MRI datasets may pose challenges in accurately classifying tumors. This study proposed a two-phase end-to-end framework comprising DenseNet-121-based deep learning to extract features and an ensemble of machine learning methodologies for precise classification. The deep learning-based feature extraction phase effectively extracted essential and discriminant features that were utilized by multiple machine learning models. Preprocessing MRI images to eliminate unwanted regions enhanced the deep learning model's feature extraction capabilities. The effectiveness of the proposed framework was evaluated by measuring the classification performance of the ensemble mechanism, which achieved an accuracy of 98.86% and an f1-score of 98.76% without any data augmentation. Notably, the random forest attained the utmost accuracy and f1-score among the machine-learning approaches used in the ensemble technique.

Keywords: Brain MRI, Multiclass, Feature extraction, Transfer learning, Ensemble learning

1 Introduction

A brain tumor is a severe type of brain disorder caused by the abnormal growth of cells within the skull. This condition is considered life-threatening and can lead to fatal consequences. Two distinct classifications exist for brain tumors, namely primary tumors and secondary tumors. It is projected that in the year 2023, approximately 18,990 individuals, comprising 11,020 males and 7,920 females, will succumb to primary malignant tumors of the brain and central nervous system (CNS) [1]. Meningioma and Pituitary tumors are the two most frequently occurring types of brain tumors. Gliomas tumors are caused by abnormal growth

in Glial cells constituting 80% of the brain. Compared to other primary tumors, this tumor has the highest mortality rate. Meningioma tumors grow in the brain and spinal cord's protective membrane, known as the meninges. However, pituitary tumors are growths that form in the pituitary gland. Pituitary tumors, though not cancerous, can cause hormonal abnormalities and irreversible visual loss [2]. Hence, it is vital for the patient's outcome to identify brain tumors in their early stages.

Brain cancers are commonly detected using three diagnostic techniques: Ultrasonography (US), Magnetic Resonance Imaging (MRI), and Computed Tomography (CT). Among these, MRI is preferred as it enables non-invasive imaging without the potentially harmful effects of radiation exposure. Moreover, by adjusting some parameters, MRI can capture various modalities such as FLAIR, T1, and T2, thereby providing additional clinical information [3].

As tumors differ in form, intensity, volume, and area, distinguishing between them can be challenging. Radiologists could benefit from assistance in effectively evaluating and segmenting images due to the complex nature of this task, which is often prone to errors. Thus, an automated computer-based method benefits tumor detection [4]. Several researchers have proposed CAD-based approaches, but traditional ML-based methods have the limitation of using hand-crafted features, which is time-consuming for larger databases [5]. Meanwhile, Deep learning, such as CNN, automates medical image analysis using automatic feature extraction from training data. This technique shows promise for brain tumor detection and classification, with researchers exploring its potential.

This study has put forth a two-phase end-to-end framework, comprising a feature extraction phase utilizing the DenseNet-121 [6] based deep learning approach and an ensemble of four machine learning approaches to ensure precise classifications. The deep learning-based feature extraction phase showcased its profound ability to extract the most distinctive and pivotal features for the purpose of accurately classifying brain tumors across a plethora of classification methods. Furthermore, this study made an invaluable contribution to the preprocessing of MRI images by eliminating superfluous regions that served as a catalyst for the deep learning model to extract discriminant features. The effectiveness of the proposed framework was unequivocally validated by the ensemble mechanism's classification performances. The GradCAM-based feature maps generated from the feature extraction phase solidified the efficiency of the proposed framework. The proposed framework attained an astounding 98.86% accuracy and 98.76% f1-score with ensemble technique, while the top performer from the individual machine learning approach is random forest which achieved 98.80% accuracy and 98.69% f1-score.

2 Related Works

Several approaches for detecting brain cancers and tumors on MRI images have been developed in recent years. These techniques primarily include classic Machine Learning and Deep Learning-based approaches.

Shah et al. [7] utilized a fine-tuned version of EfficientNet-B0 to differentiate and categorize normal and tumorous MRI images. They also improved the quality and quantity of the training samples by applying image enhancement and data augmentation. The system achieved a validation accuracy of 98.87%. The primary limitations of this study can be delineated as follows: Firstly, it solely investigated binary brain tumor classifications and neglected the more complex multi-class grades of glioma. Secondly, the model utilized in this study was fine-tuned using the image augmentation technique, which is not recommended for medical image analysis due to potential inaccuracies and errors. Sultan et al. [8] designed a computer-aided diagnosis (CAD) system to distinguish three types of brain tumor MR images along with four grades of glioma. Their method had a classification accuracy of 96.13% for the three types and 98.7% for the glioma grades. Their primary investigation(1st study) resulted in a comparatively lower accuracy when juxtaposed with the average accuracy of 96.13%. Deepak et al. [9] used CNN and SVM to categorize brain tumors with an MRI image dataset from Figshare [10]. Their method comprises two distinct phases, where the first phase involves acquiring CNN features from brain MRI images, and the second phase involves utilizing SVM to analyze the obtained features. The authors in [11] introduced a deep transfer learning framework utilizing VGG-19 for identifying three prevalent brain tumor types from MRI images. An F1-score of 94% and a high classification accuracy of 94% were attained by the proposed technique. Alanazi et al. [12] proposed a unique CNN structure comprising 22 layers that could aid in the early identification of brain tumors. An outstanding accuracy rate of 96.8% was achieved using this approach. A pre-trained GAN model applied to two datasets of MRI brain images from Nanfang Hospital and General Hospital in China and Tianjin Medical University in China between 2005 and 2010 achieved the highest accuracy of 95.60% in brain tumor segmentation, according to Ghassemi et al. [13]. This approach significantly enhanced the overall performance. One of the primary limitations of their study is the low resolution of the images generated from the GAN model.

3 Materials and Methods

The dataset underwent preprocessing and partitioning into training, validation, and testing sets. The transfer learning model based on DenseNet-121 was used to extract features from the first dense layer after training it for 100 epochs. The aforementioned features were fed into four machine learning classifiers, which were tuned using the grid search method to optimize their hyperparameters. Then, an ensemble of classifiers was devised by amalgamating all the classifiers and predicting class labels based on the majority vote. Fig. 1 illustrates the overall system architecture of this framework.

3.1 Dataset Description

The model was evaluated and analyzed using a publicly available brain tumor dataset. The dataset [14] is composed of three publicly available datasets:

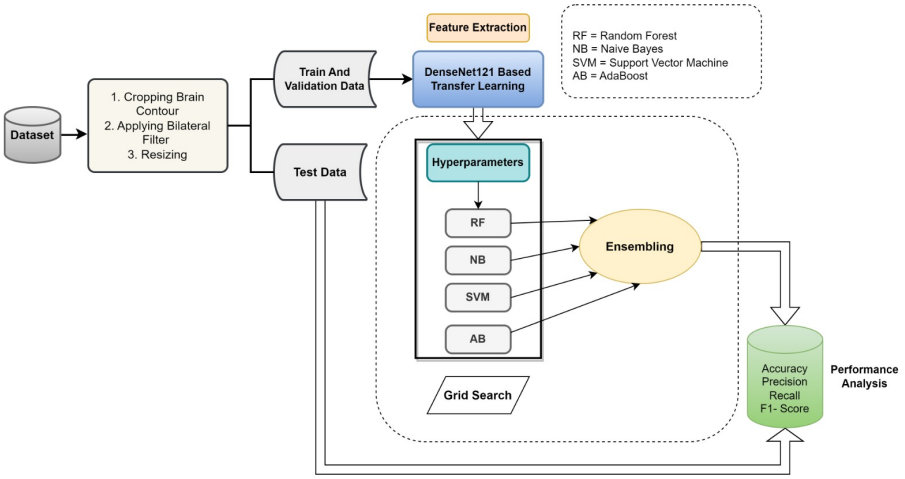


Fig. 1. A comprehensive workflow for the proposed multi-class brain MRI classification.

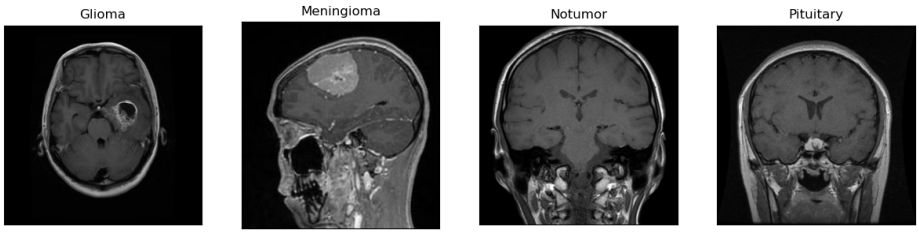


Fig. 2. Brain MRI samples with multi-class from the dataset.

Figshare [10], SARTAJ [15], and Br35H [16]. The dataset has 7023 MRI images

Table 1. Tumor type-wise breakdown of total instances in the dataset.

	Glioma	Meningioma	No-tumor	Pituitary
Train dataset	1321	1339	1595	1457
Test dataset	300	306	405	300

of the human brain. It contains four types of brain tumors: glioma, Meningioma, No-tumor, and Pituitary. The images were divided into 80% for training and 20% for validation. The dataset summary is given in Table 1. Fig. 2 demonstrates some of the images from the dataset.

3.2 Dataset Preprocessing

In brain MRI datasets, nearly all images have unwanted areas and spaces, which can lead to inaccurate classification results. Therefore, it is crucial to crop the images and keep only relevant information while removing unwanted areas. The

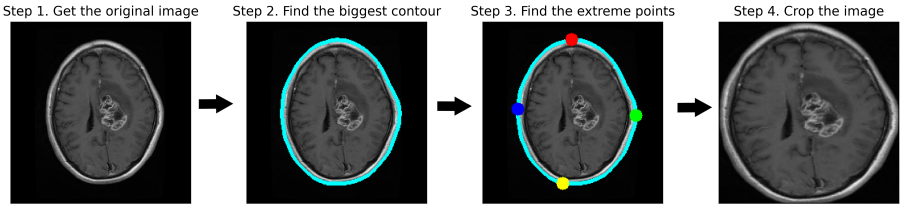


Fig. 3. Steps for cropping MRI images.

process of cropping MRI images through extreme point calculation is displayed in Fig. 3. Initially, the original MRI images are loaded for pre-processing. Then, the images are converted into binary images by applying thresholding, and image noise is removed by performing dilation and erosion operations. Next, the biggest outline of the threshold images is selected, and the four extreme points, including extreme top, bottom, right, and left, are calculated. Finally, the image is cropped using the information on contour and extreme points. Next, a bilateral filter was applied to the images, which helped to reduce noise while preserving the edges. The images were then resized to 224×224 pixels. Image augmentation was not utilized to maintain the authenticity and diversity of the MRI images used for brain tumor classification in this study. Despite its common application in enhancing data size and model generalization, its use may be limited when real-time data is necessary. The meticulous selection and preprocessing of the training data resulted in accurate outcomes on the test set.

3.3 DenseNet-121 Based Transfer Learning

DenseNet-121 [6] was used as a transfer learning model in this study. The model was trained on ImageNet [17], a dataset of over 1.4 million labeled images across 1000 different categories, covering a diverse range of objects and scenes found in real-world settings. The architecture has four dense blocks and 121 layers in total (117-conv, 3-transition, and one classification) [6]. This architecture significantly reduces the number of parameters, making it more memory-efficient than other CNN architectures while maintaining high accuracy. DenseNet-121's existing structure was insufficient for the chosen task. Therefore fine-tuning was required [18]. Before being passed into the pre-trained DenseNet-121 model, the images underwent preprocessing and resizing to $224 \times 224 \times 3$. The model's top classification layer was removed to transform it into a feature extractor for a new dataset.

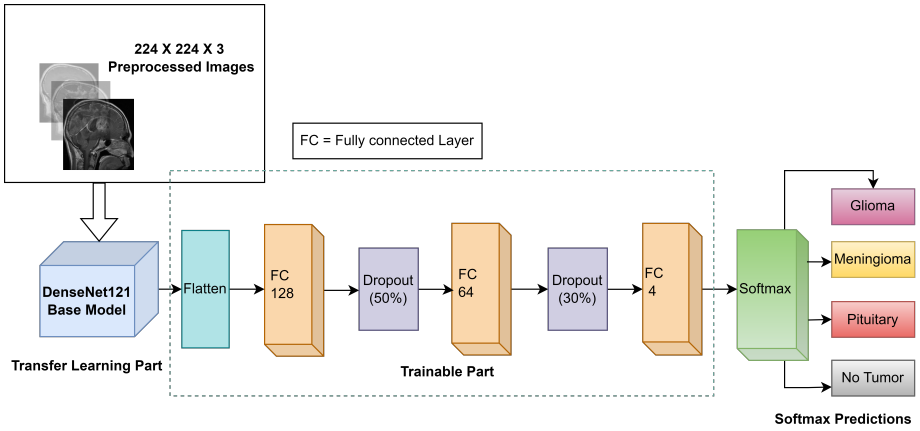


Fig. 4. DenseNet-121 transfer based feature extraction and classification technique.

The proposed transfer learning architecture with the DenseNet-121 model is depicted in Fig. 4, incorporating a flattening layer, two fully connected layers, two dropout layers, and a softmax classifier. The output of the pre-trained DenseNet-121 model was first subjected to a transformation process that converted it into a one-dimensional vector via a flattened layer. This vector was subsequently fed through a fully connected layer that comprised 128 hidden units. To mitigate overfitting, a dropout layer with a rate of 50% was introduced. A further fully connected layer with 64 units was included, with an additional dropout of 30% applied to improve model stability and generalization performance. The Softmax activation function was then incorporated, allowing the four classification labels to be generated for the target brain tumor types.

3.4 Machine Learning and Ensembling Techniques

Each individual MRI input image was processed by the trainable component of the DenseNet-121-based transfer learning model, from which 64 flattened(1-D) features of shape 1×64 were extracted from the final dense layer. These 1-D features were subsequently fed into four machine learning classifiers individually, including Gaussian Naïve Bayes [19], Adaptive Boosting [20], Random Forest [21], and Support Vector Machine [22]. Ultimately, an ensemble approach was implemented that employed the aforementioned four classifiers using the 'hard-voting' method. Grid search and five-fold cross-validation techniques were utilized to optimize the classifiers' performance. By using multiple classifiers, the accuracy of classification can be improved, as each classifier may be more sensitive to certain types of data. For a decision problem x, an ensemble model employs the hard voting rule as follows:

$$\hat{y} = max_{idx} \sum_{i=1}^{N} d_{xi} \tag{1}$$

In (1), $\hat{y}$ represents the class label that has been selected through the process of hard voting on a decision problem x, N is the number of voters (base classifiers). The classifier produces a binary vector d_{xi} with the predicted class labels for the input x. The index $\max_{idx}$ of the maximum value in the summation vector $\sum d_{xi}$ is identified. The index of the first maximum value is returned in case of multiple maxima. The class label with the most votes from the combined predictions is chosen using this technique. The ensemble technique improved performance by utilizing multiple models.

The proposed method leverages ensemble learning to enhance tumor classification accuracy, which introduces increased computational complexity compared to individual classifiers. However, this concern is alleviated by the adoption of the lightweight DenseNet-121 model as a feature extractor. With its compact and efficient architecture, DenseNet-121 significantly reduces training time and memory usage. Additionally, a streamlined majority voting approach is employed to combine predictions from multiple ML classifiers, eliminating the need for additional training or parameter estimation. As a result, the method achieves a favorable trade-off between accuracy and computational complexity, owing to the efficiency of the DenseNet-121 model.

4 Experimental Setup and Results Analysis

4.1 Training and Experimental Setup

This study employed transfer learning based on DenseNet-121, utilizing the Adam optimizer with a learning rate of 0.0001 for training. Categorical cross-entropy was used as the loss function. Four machine learning classifiers were trained using the features extracted from the transfer learning model, and their hyperparameters were fine-tuned via grid search, with the resulting values listed in Table 2. The experiment was conducted on a computer system with a 2.50 GHz Intel Core i9-11900 CPU, 32 GB memory and an NVIDIA RTX A4500 GPU with 20 GB VRAM was used for the experiments.

Table 2. Grid search results of hyperparameters optimization for multiple machine models.

ML classifiers	Hyperparameters
Random Forest	Bootstrap: True, max depth: 20, criterion: 'entropy', min samples leaf: 4, n estimators: 99
Support Vector Machine	C: 10, Kernel: rbf, Gamma: 0.01
AdaBoost	n estimators: 50
Gaussian Naïve Bayes	var smoothing: 10^{-9}

4.2 Results Analysis

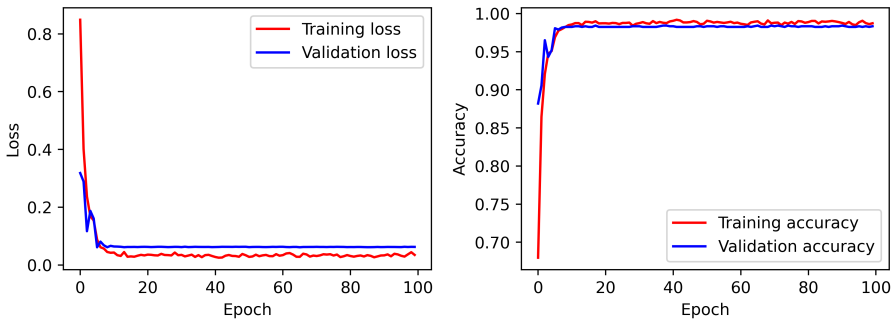


Fig. 5. Loss and accuracy curves of transfer learning(DenseNet-121).

Within this section, the experimental results and performance analysis of the proposed framework were explored. Given that the framework consisted of two distinct phases, a comprehensive analysis of the results was provided for each phase individually as well as collectively for comparison purposes. Lastly, a comparative analysis of the framework was included with recent deep learning-based research on brain tumors. Fig. 5 portrays the progression of loss and accuracy indicator curves for the training and validation collections during a period of 100 epochs. The maximum training accuracy achieved by the model was 99.19%, while the maximum validation accuracy was 98.42%. It can be inferred that effective learning of the classification of four classes, including three brain tumor types and one no tumor class, was achieved by the model. The training loss was 0.0034, and the validation loss was 0.0625. Fig. 6 illustrates Gradient Activation Maps generated by the transfer learning model, with red indicating the most influential pixels and darker shades of blue indicating the least significant. The left images indicate the original scan, the center images display the activation map, and the right images are the superimposition of the first two. The aforementioned examples serve as evidence of the effective feature extraction and classification achieved by the first phase of the proposed framework, which is based on transfer learning using DenseNet-121. Table. 3 presents the classifiers' performance across each class, evaluated using multiple metrics such as accuracy, precision, recall, F1-score, FNR (False Negative Rate), and FDR (False Discovery Rate). Incorporating FNR and FDR in evaluating the classifiers' performance is a valuable tool for identifying potential weaknesses of each classifier by providing insight into the rate of missed and false positive instances. According to the table, all classifiers achieved satisfactory results for each class. Nevertheless, the ensemble of classifiers surpassed individual classifiers by reducing false negative and false discovery rates for all classes, emphasizing the effectiveness of the proposed ensemble approach. Fig. 7 presents the confusion

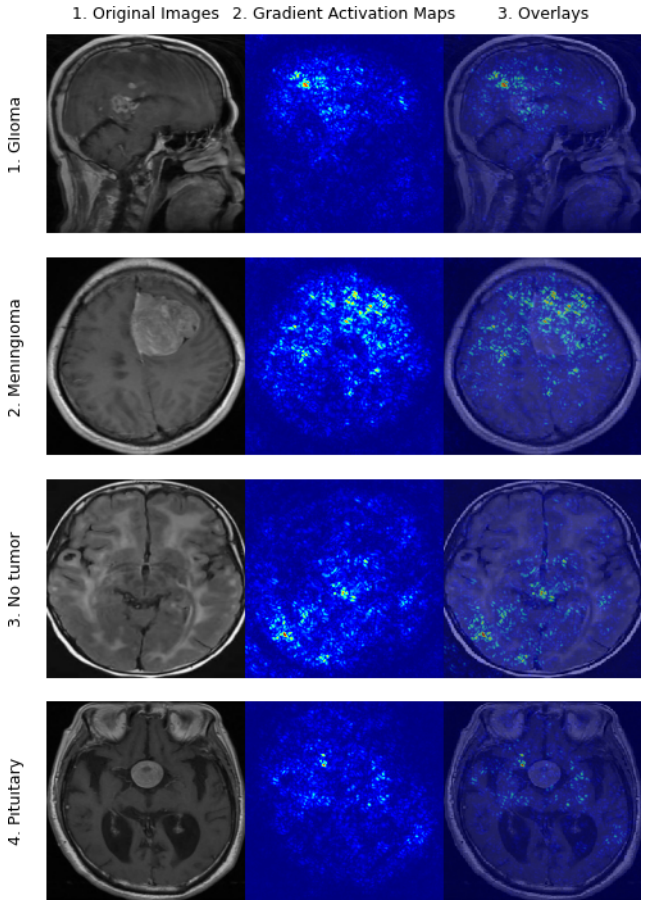


Fig. 6. Class-specific GradCAM feature maps generated from DenseNet-121 feature extraction phase.

matrix for each ML classifier. The misclassifications were 18, 19, 20, and 17 for Support Vector Machine, Gaussian Naive Bayes, AdaBoost, and Random Forest respectively.

Each classifier could precisely identify instances where there were no tumors while correctly detecting Glioma tumors posed a significant challenge for all models. The random forest algorithm emerged as the top-performing machine learning classifier for the specified task, exhibiting an impressive accuracy rate of 98.70% and the lowest misclassification rate of 1.30%. The confusion matrix for the transfer learning technique and the ensemble of classifiers is depicted in Fig. 8. The misclassification rate for the transfer learning and ensemble of classifiers was 1.22% and 1.14%, respectively. The proposed ensemble of classifiers showed promising results with no misclassification observed for the no tumor class and only 5 and 3 misclassifications observed for the Meningioma and Pi-

Table 3. Class-specific classification report for transfer learning, random forest (Individual top classifier), and the ensemble technique. FNR: False Negative Rate, FDR: False Discovery Rate.

Class	Precision(%)	Recall(%)	F1-score(%)	FNR(%)	FDR (%)
Transfer Learning					
Glioma	98.33	98	98.16	2.00	1.67
Meningioma	97.40	98.04	97.72	1.96	2.60
No tumor	100	99.75	99.88	0.25	0
Pituitary	99	99	99	1.33	1
Support Vector Machine					
Glioma	98.65	97.67	98.16	2.33	1.35
Meningioma	96.46	98.04	97.24	1.96	3.54
No tumor	99.75	99.75	99.75	0.25	0.25
Pituitary	99.33	98.67	99	1.33	0.67
Adaptive Boosting					
Glioma	99.32	97.00	98.15	3.00	0.68
Meningioma	95.85	98.04	96.93	1.96	4.15
No tumor	99.75	99.75	99.75	0.25	0.25
Pituitary	98.67	98.67	98.67	1.33	1.33
Gaussian Naive Bayes					
Glioma	98.98	96.67	97.81	3.33	1.02
Meningioma	95.56	98.37	96.94	1.63	4.44
No tumor	100	99.75	100	0	0
Pituitary	99.33	98.67	99	1.33	0.67
Random Forest					
Glioma	98.65	97.33	97.99	2.67	1.35
Meningioma	96.78	98.37	98.57	1.63	3.22
No tumor	100	100	100	0	0
Pituitary	99	98.67	98.83	1.33	1
Ensemble of Classifiers					
Glioma	98.65	97.67	98.16	2.33	1.35
Meningioma	97.10	98.37	97.73	1.63	2.90
No tumor	100	100	100	0	0
Pituitary	99.33	99	99.7	1	0.67

tuitary classes, respectively. However, the Glioma class was more challenging to predict correctly for both models than the other classes. Table. 4 showcases the precision, recall, accuracy, and F1-score of the classifiers utilized in the overall system. The results indicate that transfer learning achieved impressive performance, with a precision of 98.68%, recall of 98.70%, accuracy of 98.78%, and F1 score of 98.69%. Among the four machine learning models used, RF and SVM exhibited the highest F1 scores and were pivotal in identifying various types of brain tumors for ensembling. In this regard, the ensemble of classifiers proposed

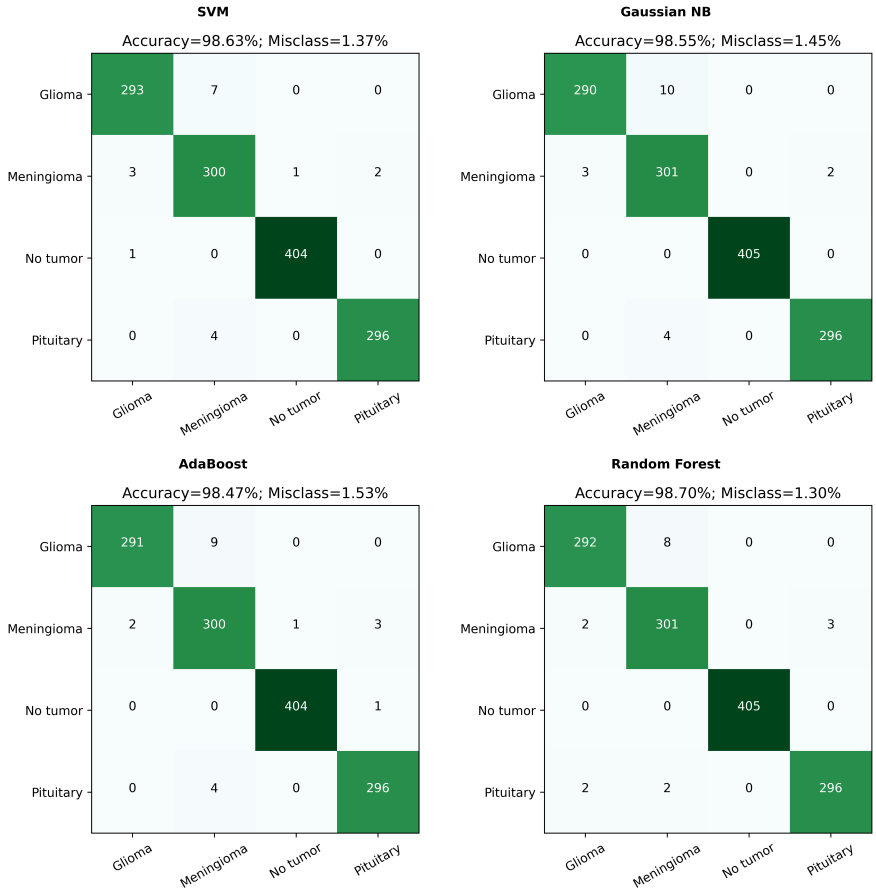


Fig. 7. Confusion matrix of four ML classifiers.

Table 4. Comparison of individual classifier performances with proposed ensemble technique: An experimental evaluation.

Model Name	Accuracy%	Precision%	Recall%	F1-Score%
DenseNet-121	98.78	98.68	98.70	98.69
SVM	98.63	98.55	98.53	98.54
RF	98.70	98.61	98.59	98.60
AB	98.47	98.40	98.36	98.37
Gaussian NB	98.55	98.47	98.42	98.44
Ensembling	**98.86**	**98.77**	**98.76**	**98.76**

in the study attained the highest values of precision (98.77%), recall (98.76%), accuracy (98.86%), and F1 score (98.76%). These results are visually represented in Fig. 9 which displays a comparison bar chart of the metrics mentioned ear-

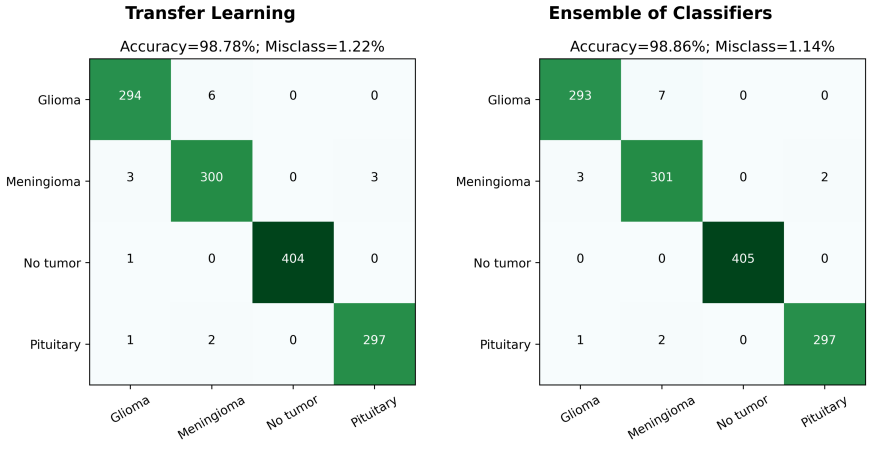


Fig. 8. Confusion matrix of Transfer learning and Ensemble of classifiers.

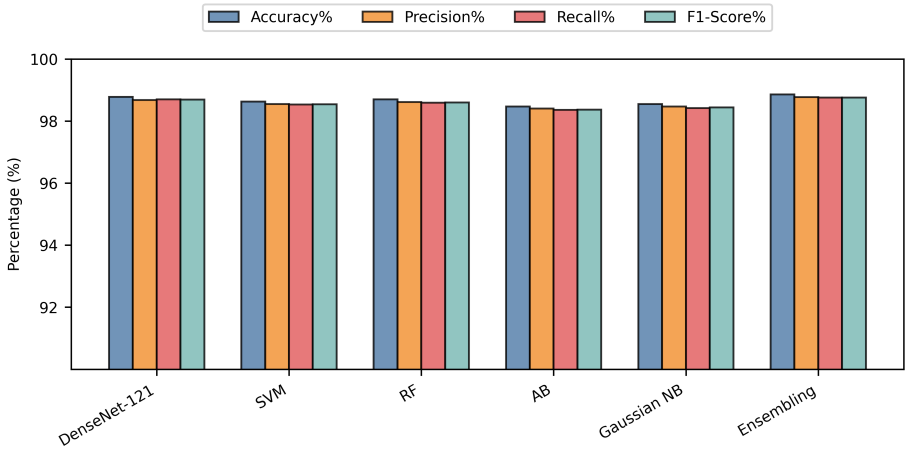


Fig. 9. Graphical Representation of the performance of each model used in this study.

lier. Overall, the findings suggest that the proposed ensemble approach has the potential to enhance the accuracy and effectiveness of automated brain tumor diagnosis. A comparison of the performance of the suggested framework and that of previous research in the field of automated detection of brain tumors is given in Table 5. The results show that the suggested framework achieved

Table 5. Comparison of brain tumor classification performance with recent studies.

Authors	Classification Type	Approach	Data Augmentation	Major findings (best results)
Shah et al.[7]	Binary	Fine tuned EfficientNet-B0	Yes	Acc: 98.87%
Sultan et al.[8]	Multi	Custom CNN	Yes	Acc: 98.7%
Deepak et al.[9]	Multi	CNN and SVM	No	Acc: 95.82%
Mondal et al.[11]	Multi	Transfer Learning	Yes	Acc: 94% F1-score: 94%
Alanazi et al.[12]	Multi	Transfer Learning	No	Acc: 96.90%
Ghassemi et al. [13]	Multi	GAN	Yes	Acc: 95.60%. F1-score: 95.10%
Proposed	**Multi**	**Trasnfer Learning+ Ensemble of ML classifiers**	**No**	**Acc: 98.86%. F1-score: 98.73%**

better outcomes than all other studies that worked on multiclass classification. This implies that the suggested approach has significant potential for practical application in automated brain tumor diagnosis.

5 Conclusion and Future Works

Brain tumors endanger the well-being of a person, and manual detection demands a lot of time and the expert knowledge of a radiologist. This study proposed a comprehensive, two-phase end-to-end framework that incorporated a feature extraction phase based on DenseNet-121 transfer learning, followed by an ensemble of four distinct machine learning techniques to enable highly accurate classification. The deep learning-based feature extraction phase was capable of extracting discriminative and salient features, enabling precise classification of brain tumors through multiple ML classification methods. Notably, the proposed framework leveraged GradCAM-based feature maps generated during the feature extraction phase, providing compelling evidence for the efficiency and efficacy of the feature extraction process. These deep features were then fed into

four machine-learning classifiers. The optimal hyper-parameters of each classifier were fine-tuned using the grid search technique. An ensemble that utilizes majority voting to predict class labels was developed by integrating all the classifiers. The proposed framework showed an exceptional ability to precisely classify three different tumor types and normal MRI brain images, achieving an outstanding classification accuracy of 98.86%. Again, the high precision rate of 98.77%, recall rate of 98.76%, and F1-score of 98.76% further emphasized its proficiency and adaptability, highlighting its potential in various applications. The framework achieved this outcome without data augmentation techniques, which is remarkable. This implies that the framework depended on its resilience and adaptability rather than artificially enhancing the dataset's size or variety. However, this technique may have restricted applicability to other forms of medical imaging besides MRI scans, which is a limitation of this study. The proposed model demonstrated higher prediction accuracy for the Meningioma, Pituitary and Normal class than the Glioma class, which is a limitation. Attention mechanisms can be utilized to enhance feature extraction to overcome this issue in the future. Moreover, the performance of this study can be evaluated on other large medical imaging datasets to increase its effectiveness and reliability for real-time detection and classification.

References

1. American Society of Clinical Oncology: Brain tumor statistics (2023). URL https://www.cancer.net/cancer-types/brain-tumor/statistics. Accessed on April 6, 2023
2. Komninos, J., Vlassopoulou, V., Protopapa, D., Korfias, S., Kontogeorgos, G., Sakas, D.E., Thalassinos, N.C.: Tumors metastatic to the pituitary gland: case report and literature review. The Journal of Clinical Endocrinology & Metabolism **89**(2), 574–580 (2004)
3. Bauer, S., Wiest, R., Nolte, L.P., Reyes, M.: A survey of mri-based medical image analysis for brain tumor studies. Physics in Medicine & Biology **58**(13), R97 (2013)
4. Reddy, A.V., Krishna, C.P., Mallick, P.K., Satapathy, S.K., Tiwari, P., Zymbler, M., Kumar, S.: Analyzing mri scans to detect glioblastoma tumor using hybrid deep belief networks. Journal of Big Data **7**, 1–17 (2020)
5. Khalid, S., Khalil, T., Nasreen, S.: A survey of feature selection and feature extraction techniques in machine learning. In: 2014 science and information conference, pp. 372–378. IEEE (2014)
6. Huang, G., Liu, Z., Van Der Maaten, L., Weinberger, K.Q.: Densely connected convolutional networks. In: Proceedings of the IEEE conference on computer vision and pattern recognition, pp. 4700–4708 (2017)
7. Shah, H.A., Saeed, F., Yun, S., Park, J.H., Paul, A., Kang, J.M.: A robust approach for brain tumor detection in magnetic resonance images using finetuned efficientnet. IEEE Access **10**, 65,426–65,438 (2022)
8. Sultan, H.H., Salem, N.M., Al-Atabany, W.: Multi-classification of brain tumor images using deep neural network. IEEE access **7**, 69,215–69,225 (2019)
9. Deepak, S., Ameer, P.: Automated categorization of brain tumor from mri using cnn features and svm. Journal of Ambient Intelligence and Humanized Computing **12**, 8357–8369 (2021)

10. Cheng, J.: brain tumor dataset (2017). DOI 10.6084/m9.figshare.1512427.v5. URL https://figshare.com/articles/dataset/brain_tumor_dataset/1512427. Accessed on March 6, 2023
11. Mondal, M., Faruk, M.F., Raihan, N., Ahammed, P.: Deep transfer learning based multi-class brain tumors classification using mri images. In: 2021 3rd International Conference on Electrical & Electronic Engineering (ICEEE), pp. 73–76. IEEE (2021)
12. Alanazi, M.F., Ali, M.U., Hussain, S.J., Zafar, A., Mohatram, M., Irfan, M., AlRuwaili, R., Alruwaili, M., Ali, N.H., Albarrak, A.M.: Brain tumor/mass classification framework using magnetic-resonance-imaging-based isolated and developed transfer deep-learning model. Sensors **22**(1), 372 (2022)
13. Ghassemi, N., Shoeibi, A., Rouhani, M.: Deep neural network with generative adversarial networks pre-training for brain tumor classification based on mr images. Biomedical Signal Processing and Control **57**, 101,678 (2020)
14. Nickparvar, M.: Brain tumor mri dataset (2021). DOI 10.34740/KAGGLE/DSV/2645886. URL https://www.kaggle.com/dsv/2645886. Accessed on March 6, 2023
15. Bhuvaji, S., Kadam, A., Bhumkar, P., Dedge, S., Kanchan, S.: Brain tumor classification (mri) (2020). DOI 10.34740/KAGGLE/DSV/1183165. URL https://www.kaggle.com/dsv/1183165. Accessed on March 6, 2023
16. Hamada, A.: Br35h:: Brain tumor detection 2020. URL https://www.kaggle.com/datasets/ahmedhamada0/brain-tumor-detection
17. ImageNet: *ImageNet* (2020). "http://www.image-net.org/ [accessed January 19, 2020]
18. Tajbakhsh, N., Shin, J.Y., Gurudu, S.R., Hurst, R.T., Kendall, C.B., Gotway, M.B., Liang, J.: Convolutional neural networks for medical image analysis: Full training or fine tuning? IEEE transactions on medical imaging **35**(5), 1299–1312 (2016)
19. John, G.H., Langley, P.: Estimating continuous distributions in bayesian classifiers. arXiv preprint arXiv:1302.4964 (2013)
20. Freund, Y., Schapire, R.E.: A decision-theoretic generalization of on-line learning and an application to boosting. Journal of computer and system sciences **55**(1), 119–139 (1997)
21. Breiman, L.: Random forests. Machine learning **45**, 5–32 (2001)
22. Cortes, C., Vapnik, V.: Support-vector networks. Machine learning **20**, 273–297 (1995)